Advances in Nonlinear Variational Inequalities
ISSN: 1092-910X
Vol 26 No. 4 (2023)

Bioconvection of a Radiating Hybrid Nanofluid Past Over a Thin Needle in the Presence of Various Chemical Reaction

Arindam Das, Tapas Datta,Arijit Mandal,

Assistant Teacher of Mathematics, Bhubanmayee Jr. High School, Pandapara Kalibari, Jalpaiguri,735132, West Bengal, India

Department of Mathematics, Aghore Kamini Prakash Chandra Mahavidyalaya, Bengai, Hooghly, West Bengal - 712611

Assistant Teacher, Buridaha Primary School, Buridaha, Dighalbar, Gazole, Malda, West Bengal -732138

Article History:

Received: 06-10-2023

Revised: 21-11-2023

Accepted: 29-11-2023

Abstract: The photograph reactant nature of TiO2 tracks down applications in restorative field to dispense with malignant growth cells, microbes, and infections under gentle bright enlightenment and the antibacterial quality of Ag makes the arrangement Ag+TiO2 pertinent for different purposes. It can likewise be utilized in other designing machines and businesses like mugginess sensor, coolants, and in footwear industry. Thus, this study manages the examination of the impacts of attractive field and warm radiation in Casson liquid progression of electrically directing Ag+TiO2/H2O half breed nanofluid. Besides, the gyrotactic microorganisms are utilized as dynamic blenders to forestall agglomeration and sedimentation of TiO2 that happens because of its hydrophobic nature. The numerical model appears as incomplete differential conditions with consistency and warm conductivity being the elements of volume division. These conditions are switched over completely to conventional differential conditions by utilizing similitude change and are addressed by RKF-45 technique with the guide of shooting strategy. It is seen that the expansion in the size of the needle upgrades the general exhibition of the cross breed nanofluid. Moreover, the temperature of the mixture nanofluid elevates with the expansion in volume part. It is seen that the contact delivered by the Lorentz force builds the temperature of the nanofluid.

Keywords: thin needle, radiating hybrid nanofluid, gyrotactic microorganisms, Casson fluid, magnetic field

INTRODUCTION:

Bioconvection is a collective behaviour of microorganisms leading to pattern or structure in certain microbial suspensions. Microorganisms are classified into several categories: one such category is "extreme psychrophiles" (which grow at temperatures below 0°C), others include "thermophiles," which survive within a temperature range of 50–80°C, and another class includes the hyperthermophiles that resist reasonable high levels from 65* to approx.120*C) and so forth; depending on preferred environmental conditions; different species would belong in contending classes. The phenomenon of the formation Benard cells (polygonal convection patterns) associated with motion in such ciliates was first noted by Platt [1], a fact that led him to introduce the term bioconvection. Ghorai and Slope [2] investigated the patterning in microbial suspension, discussing a possible mechanism of their formation.

The first scheme was originally suggested, by Choi and Eastman [3], in which nanometer-sized metal particles are dispersed into conventional fluids to improve the thermal conductivity; these types of fluid are called as 'nanofluids'. The research on nanofluids has emerged as an exciting field, mainly to improve heat transfer properties of working fluids for many industrial applications. Xuan et al. Research conducted by Das et al. [4,5] on heat transfer capability as a function of nanoparticle dispersion explained that nanofluids can be used in cooling systems and soap production due to the amount of heat transferred from one place to another quickly, while research also demonstrated applications could revolve around medical procedures (such as radio frequency tumor ablation), nuclear reactors or semiconductor technology within CPU manufacture etc.

The application of magnetic fields to nanofluids was attempted by Sinha and Misra [6], and this study was extended to bionanofluids by Basir et al. [7]. Applications of magnetonanofluids include MHD pumps, gas turbines, cancer treatment, hyperthermia therapy, magnetic resonance imaging, sterilization devices, and blockage removal in conduits. For further information regarding these apps, check [8-13].Nanofluids also hold promise in microfluidic devices where conventional mixing techniques have been challenging to implement. The bio-applications may be adverse due to joule heating arising from a conventional mixer. In this regard, Kuznetsov proposed motile microorganisms as an alternative to dynamic mixers. Self-propelling microorganisms serve to enhance the mix of nanoparticles in the fluid to cause bioconvection-a collective movement phenomenon. The research of Kuznetsov extended from bioconvection to thermo-bioconvection [15-17], which has demonstrated temperature gradients imposed on bioconvective patterns.

Aziz et al. [18] have studied the dynamics of nanofluids flow in the presence of gyrotactic microorganisms, while Tham et al. [19,20] have pointed to the relevance of bioconvection in microfluidic systems. Shaw et al. [21] have deduced that in nanofluids, the heat transfer is greatly influenced by thermophoresis and Brownian motion. Furthermore, a rise in viscosity of the base fluid due to suspension of microorganisms was noticed by Khan and Makinde [24,25]. Gireesha et al. [26,27] presented the three-dimensional bioconvective flow considering the effects of Brownian motion and thermophoresis.

All these studies have motivated applications of bioconvection in biomicrosystems, biomedical applications, microfluidic devices, fuel cells, wastewater treatment, and in the production of alcohol and bakery products. A combination of bioconvection with nanofluids opens bright avenues for the enhancement of fluid dynamics and process efficiency in these wide areas.

Due to inherently of single-component nanoparticles and their limitations it becomes very hard sometimes impossible that they meet up particular requirement. A prominent example is Al_2O_3, which is very stable and chemically inert but has low thermal conductivity. Carbon nanoparticles exhibit poor current conductivity associated with hybrid ones like Al, Ag and Cu which are thermally conductive but most of them are instable in nature as well as chemically active. In fact, in order to avoid the above mentioned limitations a new generation of hybrid nanofluids were prepared by mixing nanoparticles with different physical-chemical natures with each other thus adding value for their optimal performance corresponding to application

interest. Changing NPs in Stability Hybrid nanofluids were prepared by mixing two different types of nanoparticles suspended in a host fluid. The synergistic effect of different nanoparticles leads to increased heat transfer coefficient in these hybrid nanofluids. Hayat, Nadeem, et al. [28] also concluded that hybridization of the fluid greatly improved heat transfer rate against pure paradoxical magnitude hyperbolic functions with exponential density in presence of binary chemical reaction.). Similarly, Chamkha et al. a investigated the natural convection in a rectangular enclosure of hybrid nanofluids with magnetic fieldsuet al. When Manjunatha et al. When the fluid flow characteristics of Cu-Al_2O_3/H_2O hybrid nanofluid were investigated by Bianco et al. [32], they found various improving viscosity and their influence on the flowconduct.

The extremely thin fluid layer covering a body where the flow rapidity escalations from zero at the surface to the free-stream value is referred to as a "boundary layer" in fluid dynamics.

It was Ludwig Prandtl who originally presented this idea. In fluid flows that preserve axisymmetry, such thin needles typically have boundary layers that are far smaller than the needle's size. In medicinal contexts, such blood flow in veins and disease dissemination inside the body, to name just two examples, such flows have numerous practical applications. In industrial contexts, they are useful for wind engineering and water flow in maritime environments.The early studies of Newtonian fluid flow over slender needles were made by Lee [33, 39]. Narain and Uberoi [34, 35, 40, 41] later studied the convection phenomena around needles. Chen and Smith [42] investigated the effects of surface heat flux and wall temperature on the flow around non-isothermal needles. Free-stream flow over a needle was examined by Ishak et al. [43], followed by extension to both aiding and opposing flows of nanofluids by Ahmad et al. [44]. Grosan and Pop [45] conducted a mathematical analysis of the forced convection of Cu/H_2O and Al_2O_3/H_2O nanofluids over non-isothermal needle surfaces based on the Tiwari-Das model. Finally, Hayat et al. [46] analyzed heat transfer through CNTs in needle flow with variable heat flux.

Ag incorporation into TiO_2 results in a hybrid photocatalyst with enhanced antibacterial activity. Indeed, it has been reported that the addition of Ag enhances the photocatalytic activity of TiO_2 under UV irradiation by reducing the recombination rate of photoinduced charge carriers, increasing the quantity of hydroxyl radicals and other generated reactive oxygen species. Indeed, this effect has been documented to enhance the photocatalytic degradation rate of certain contaminants, like Rhodamine, under visible light at a 0.15% doping concentration of Ag in TiO_2 [49]. Moreover, the plasmonic capabilities of these Ag+TiO_2 composites are being combined with optical fibers for a number of different applications, including in humidity sensing.

Axisymmetric flow of nanofluids around slender needles is an issue of great importance in many medical and industrial processes. Vaccines are usually prepared in liquid media containing weakened pathogens; these have to get their sites of action by passing through different body liquids with various conditions. It is envisioned that microorganisms face laminar and turbulent flows in order to optimize their growth and bioprocesses in continuous stirred tank bioreactors and photobioreactors. Magnetic fields and biodynamic mixers can be

applied to surmount some problems such as nanoparticle agglomeration and deposition. Special properties possessed by Ag+TiO_2/H_2O hybrid nanofluids and behavior in magnetic fields and thin needle conditions merit further investigation with a view to improving their applicability in both medical and industrial applications.

Present research emphasizes the development of understanding and optimization of hybrid nanofluids' behavior for applications where conventional mixing techniques do not give satisfaction. The utilization of biodynamic mixers and magnetic fields presents an attractive proposition toward enhancement in the efficiency and efficacy of nanofluid-based processes.

5.1 MATHEMATICAL FORMULATION:

Consider a two layered progression of half breed nanofluid past a slender needle of range r=R(x). The limit layer is thought to be moving with uniform speed U_w in the equivalent or inverse heading of the free stream of the uniform speed U_{in}.

Table 1: Characteristics of Nanofluids and Hybrids.

Properties	Nanofluid	Hybrid nanofluid
Density $\left(kg.m^{-3}\right)$	$\rho_{nf}=\left(1-\varphi\right)\rho_{bf}+\varphi\rho_{np}$	$\rho_{hnf}=\left(1-\varphi_2\right)\left(\begin{matrix}\left(1-\varphi_1\right)\rho_{bf}\\+\varphi_1\rho_{np1}\end{matrix}\right)+\varphi_2\rho_{np2}$
Heat capacity $\left(J.kg^{-1}.\mathrm{K}^{-1}\right)$	$\left(\rho c_p\right)_{nf}=\left(1-\varphi\right)\left(\rho c_p\right)_{bf}+\varphi\left(\rho c_p\right)_{np}$	$\left(\rho c_p\right)_{hnf}=\left(1-\varphi_2\right)\left(\begin{matrix}\left(1-\varphi_1\right)\left(\rho c_p\right)_{bf}\\+\varphi_1\left(\rho c_p\right)_{np1}\end{matrix}\right)$ $+\varphi_2\left(\rho c_p\right)_{np2}$
Viscosity $\left(\mathrm{N.m}^{-2}\right)$	$\mu_{nf}=\frac{\mu_{bf}}{\left(1-\varphi\right)^{2.5}}$	$\mu_{hnf}=\frac{\mu_{bf}}{\left(1-\varphi_1\right)^{2.5}\left(1-\varphi_2\right)^{2.5}}$
Thermal conductivity $\left(\mathrm{W.m}^{-1}.K^{-1}\right)$	$\frac{\kappa_{nf}}{\kappa_{bf}}=\frac{\kappa_{np}+2\kappa_{bf}-2\varphi\left(\kappa_{bf}-\kappa_{np}\right)}{\kappa_{np}+2\kappa_{bf}+\varphi\left(\kappa_{bf}-\kappa_{np}\right)}$	$\frac{\kappa_{hnf}}{\kappa_{nf}}=\frac{\kappa_{np2}+2\kappa_{nf}-2\varphi_2\left(\kappa_{nf}-\kappa_{np2}\right)}{\kappa_{np2}+2\kappa_{nf}+\varphi_2\left(\kappa_{nf}-\kappa_{np2}\right)}$, $\frac{\kappa_{nf}}{\kappa_{bf}}=\frac{\kappa_{np1}+2\kappa_{bf}-2\varphi_1\left(\kappa_{bf}-\kappa_{np1}\right)}{\kappa_{np1}+2\kappa_{bf}+\varphi_1\left(\kappa_{bf}-\kappa_{np1}\right)}$
Electrical conductivity $\left(\mathrm{S.m}^{-1}\right)$	$\frac{\sigma_{nf}}{\sigma_{bf}}=\frac{\sigma_{np}+2\sigma_{bf}-2\varphi\left(\sigma_{bf}-\sigma_{np}\right)}{\sigma_{np}+2\sigma_{bf}+\varphi\left(\sigma_{bf}-\sigma_{np}\right)}$	$\frac{\sigma_{hnf}}{\sigma_{nf}}=\frac{\sigma_{np2}+2\sigma_{bf}-2\varphi_2\left(\sigma_{bf}-\sigma_{np2}\right)}{\sigma_{np2}+2\sigma_{bf}+\varphi_2\left(\sigma_{bf}-\sigma_{np2}\right)}$, $\frac{\sigma_{nf}}{\sigma_{bf}}=\frac{\sigma_{np1}+2\sigma_{bf}-2\varphi_1\left(\sigma_{bf}-\sigma_{np1}\right)}{\sigma_{np1}+2\sigma_{bf}+\varphi_1\left(\sigma_{bf}-\sigma_{np1}\right)}$

In the event that the surface temperature of the needle T_w is thought to be more noteworthy than the surrounding temperature T_{in} then it compares to a warmed needle and the condition $T_w < T_{in}$ relates to a cooled needle. In this review, this temperature distinction is thought to be unimportant. It is expected that the grouping of suspended nanoparticles is weaken for the counteraction of the bioconvection insecurity.

The nanoparticles are suspended utilizing surfactants, with the goal that it forestalls the agglomeration and surface strain among water and nanoparticles. Water, an optically thick medium is decided to be the base liquid as it gives a climate that is the most appropriate for the consistently conveyed gyrotactic microorganisms to make due. This study expects round shape for the suspended nanoparticles.

Nanoparticle clumping may be mitigated by including synthetic chemicals or microbes that act as dynamic blenders. Not only is it wasteful to employ dynamic blenders as additives, but they also don't safeguard the equipment.

So, it's best to avoid using genetically engineered germs and instead rely on naturally occurring bacteria. Due to their density relative to their surrounding media, these microbes will naturally gravitate towards the bottom of the cycling container. An exciting finding that these microbes made was that they move in a given direction in response to stimulus [50]. Microbes are subjected to various treatments in response to this, including gravities, phototaxis, magneto taxis, chemo tax, ELT gyratory, and so on. The mobility of these bacteria is affected by a combination of factors, including gravity, light, magnetic field (attractive), material species (chemicals), and mass angle. In this research, scaffolds are used to place gyrotactic microorganisms. These organisms move based on the principle of mass segregation rather than increased density since they do not need more energy to move.

Subsequently, involving these microorganisms as dynamic blenders is affordable and productive. The microorganism's movement in the nanofluid can be approximated as

$$m = M\mu + M\mu' - D_M \nabla M \qquad (01)$$

Where $\mu' = \left(\frac{bW_c}{\Delta C}\right)\nabla C$. Here, both ∇C and changes in the centralization of the mass liquid ΔC , are viewed as in the model because of the reality these microorganisms move in the homogeneous mass liquid during bioconvection.

A magnetic field B_0 is applied opposite to the progression of the electrically leading crossover nanofluid. The connection of attractive field with the actuated current J and the Lorentz force f is characterized as

$$f = J \times B = \sigma_{hnf} B_0^2 \left(v_x - U_{in}\right) \qquad (02)$$

Table 2: Thermophysical characteristics of both nanoparticles and base fluid[47]

	$\rho\left(kg.m^{-3}\right)$	$\sigma\left(S.m^{-1}\right)$	$\kappa\left(W.m^{-1}.K^{-1}\right)$	$c_p\left(\mathrm{J.kg^{-1}}.K^{-1}\right)$
H_2O	997.1	5.5×10^{-6}	0.6071	4179
Ag	10490	63×10^{6}	429	235
TiO_2	4250	2.4×10^{6}	8.953	686.2

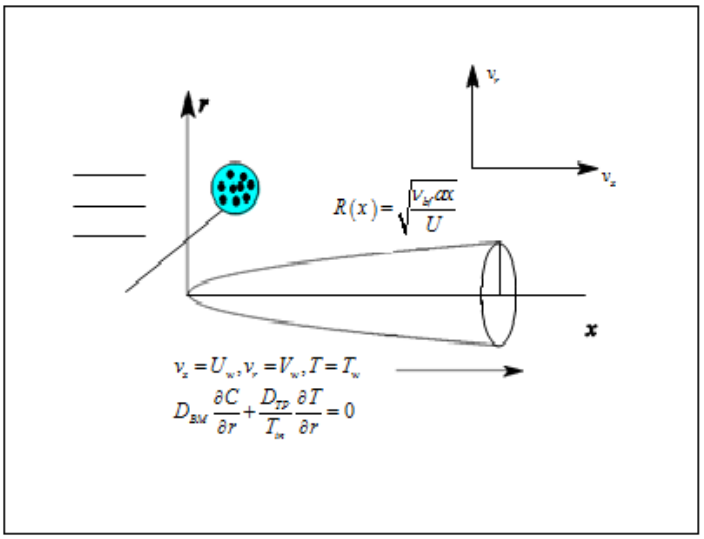

Figure 01: Physical flow model

The overseeing conditions in needle shaped are organized for the progression of crossover nanofluid past a meager needle are communicated as [38, 50]. The thermophysical properties are characterized in (Table 1) and their actual constants are yielded (Table 2)

$$\left.\begin{aligned}
&\frac{\partial}{\partial x}\left(rv_x\right)+\frac{\partial}{\partial r}\left(rv_r\right)=0\\
&v_x\frac{\partial v_x}{\partial x}+v_r\frac{\partial v_x}{\partial r}=\left(1+\frac{1}{\beta}\right)\frac{\nu_{hnf}}{r}\frac{\partial}{\partial r}\left(r\frac{\partial v_x}{\partial r}\right)-\frac{\sigma_{hnf}B_0^2}{\rho_{hnf}}\left(v_x-U_{in}\right)\\
&v_x\frac{\partial T}{\partial x}+v_r\frac{\partial T}{\partial r}=\frac{\kappa_{hnf}}{\left(\rho c_p\right)_{hnf}}\frac{1}{r}\frac{\partial}{\partial r}\left(r\frac{\partial T}{\partial r}\right)+\tau\left\{D_{BM}\frac{\partial T}{\partial r}\frac{\partial C}{\partial r}+\frac{D_{TP}}{T_{in}}\left(\frac{\partial T}{\partial r}\right)^2\right\}+\frac{1}{\left(\rho c_p\right)_{hnf}}\frac{\partial q_r}{\partial r}\\
&v_x\frac{\partial C}{\partial x}+v_r\frac{\partial C}{\partial r}=\frac{D_{BM}}{r}\frac{\partial}{\partial r}\left(r\frac{\partial C}{\partial r}\right)+\frac{D_{TP}}{T_{in}}\frac{1}{r}\frac{\partial}{\partial r}\left(r\frac{\partial T}{\partial r}\right)\\
&v_x\frac{\partial M}{\partial x}+v_r\frac{\partial M}{\partial r}=\frac{D_{MO}}{r}\frac{\partial}{\partial r}\left(r\frac{\partial M}{\partial r}\right)-\left(\frac{bW_c}{\Delta C}\right)\frac{1}{r}\frac{\partial}{\partial r}\left(M\frac{\partial C}{\partial r}\right)
\end{aligned}\right\}$$

(02)

With the appropriate boundary conditions are

$$\left.\begin{array}{l} v_x = U_w, v_r = V_w, T = T_w, D_{BM}\dfrac{\partial C}{\partial r} + \dfrac{D_{TP}}{T_{in}}\dfrac{\partial T}{\partial r} = 0, M = M_w \ at\ r = R(x) \\ v_x \to U_{in}, T \to T_{in}, C \to C_{in}, M \to M_{in} \ as\ r \to \infty \end{array}\right\} \quad (03)$$

Heat transfer studies involving radiation effects generally formulate the energy equation by the use of Rosseland approximation provided in Equation (02). The Rosseland approximation is one way of simplifying the highly complicated interactions of thermal radiation in a fluid to a form that may include the effects of radiation in models having heat transfer.

To begin, we will determine the two most basic dimensionless factors related to radiation impacts on heat transfer and fluid flow: the Planck number and the optical thickness. The Planck number is a dimensionless number to identify the importance of radiation compared with conduction for a given system. The optical thickness identifies a medium as transparent, semitransparent, or opaque, showing how effectively the medium interacts with the thermal radiation.

Therefore, in applying the Rosseland approximation, a few simplifications in treating the problem of radiative heat transfer can be made. Because the Rosseland approximation averages radiative heat flux over the wavelength spectrum, it produces more accurate but simpler energy equations. This affects the appearance of the Planck number and optical thickness as distinct parameters in the final equations. A new dimensionless parameter, called the radiation parameter or radiation boundary, is introduced in place of these parameters.

It incorporates the previously listed parameters. This radiation parameter, defined based on Planck number and optical thickness, effectively can represent a compact form of the two factors' coupled effects on thermal radiation within a system. It now provides an easier way of considering the effects of radiation during heat transfer without necessarily having to deal with all of the complexities separately brought about by the Planck number and optical thickness.

To put it another way, the Rosseland approximation makes it easier to model thermal problems involving radiation heat transfer effects by combining the effects of the Planck number and optical thickness into a single general radiation parameter. This makes it possible to analyze and compute radiation effects in these kinds of heat transfer problems more easily, and the models it uses are still reasonably accurate while still being practical.

$$q_r = -\frac{4\sigma^*}{3k}\frac{\partial T^4}{\partial r} \quad (04)$$

This guess incorporates dissemination term that was presented in light of the hypothesis of preservation of energy. Since the temperature distinctions between T_w and T_∞ is thought to be essentially little, the Rosseland guess can be linearized by growing T^4 as per the Taylor series about T_{in} . The decreased development subsequent to dismissing the higher request terms is

$$T^4 = 4T_{in}^3 T - 3T_{in}^4 \tag{05}$$

By using this expression, the energy Eq. in (02) reduces to

$$v_x \frac{\partial T}{\partial x} + v_r \frac{\partial T}{\partial r} = \frac{\kappa_{hnf}}{\left(\rho c_p\right)_{hnf}} \frac{1}{r} \frac{\partial}{\partial r}\left(r \frac{\partial T}{\partial r}\right) + \tau \left\{ D_{BM} \frac{\partial T}{\partial r} \frac{\partial C}{\partial r} + \frac{D_{TP}}{T_{in}} \left(\frac{\partial T}{\partial r}\right)^2 \right\} + \frac{16\sigma^* T_{in}^3}{3k\left(\rho c_p\right)_{hnf}} \frac{\partial^2 T}{\partial r^2} \tag{06}$$

The following similarity transformation transforms the partial differential equations to ordinary differential equations:

$$\xi = \frac{Ur^2}{\nu_{bf} x}, \omega = \nu_{bf} x f'(\xi), U = U_w + U_{in}, \vartheta(\xi) = \frac{T - T_{in}}{T_w - T_{in}},$$

$$h(\xi) = \frac{C - C_{in}}{C_w - C_{in}}, m(\xi) = \frac{M - M_{in}}{M_w - M_{in}} \tag{07}$$

The stream capability ω is characterized as $v_x = \frac{1}{r}\frac{\partial \omega}{\partial r}$ and $v_r = -\frac{1}{r}\frac{\partial \omega}{\partial x}$, where v_x is the axial speed part and v_r is the radial speed part. If $\xi = a$ is a consistent relating to the outer layer of upset alluding to the mass of the needle then setting $\xi = a$ in Eq. (02) gives $R(x) = \sqrt{\frac{\nu_{bf} ax}{U}}$ that depicts the shape and size of the body width and its surface. The local skin friction coefficient, local Nusseltnumber, local Sherwood number and local microorganism number are defined as

$$\left.\begin{aligned} Cf_x &= \frac{2\mu_{hnf}}{\rho U^2}\left(\frac{\partial v_x}{\partial r}\right)_{r=R(x)}, Nu_x = -\frac{x\kappa_{hnf}}{T_w - T_{in}}\left(\left(\frac{\partial T}{\partial r}\right)_{r=R(x)} + q_r\right) \\ Sh_x &= -\frac{xD_{BM}}{C_w - C_{in}}\left(\frac{\partial C}{\partial r}\right)_{r=R(x)}. Nm_x = -\frac{xD_{MO}}{M_w - M_{in}}\left(\frac{\partial M}{\partial r}\right)_{r=R(x)} \end{aligned}\right\} \tag{08}$$

The continuity Eq. in (02) is satisfied for the above-mentioned transformation and the transformed systems of equations are

$$\left.\begin{aligned} &2\frac{\mu_{hnf}}{\mu_{bf}}\left(1+\beta^{-1}\right)\left(\xi f''\right)' + \frac{\rho_{hnf}}{\rho_{bf}} ff' - \frac{\sigma_{hnf}}{\sigma_{bf}} M_F\left(f' - \delta\right) = 0 \\ &\frac{\kappa_{hnf}}{\kappa_{bf}}\frac{1}{Pr}\left(2 + RD\right)\left(\xi\vartheta'\right)' + \frac{\left(\rho c_p\right)_{hnf}}{\left(\rho c_p\right)_{bf}}\left[f\vartheta' + 2\xi\left(N_{BM}\vartheta' h' + N_{TP}\left(\vartheta'\right)^2\right)\right] = 0 \\ &2\left(\xi h'\right)' + Le.fh' + 2\frac{N_{TP}}{N_{BM}}\left(\xi\vartheta'\right)' = 0 \\ &2\left(\xi m'\right)' + Pr.Lb.fm' - Pe\left[2\xi\left(m'h' + mh'' + \Upsilon h''\right) + \left(m + \Upsilon\right)h\right] = 0 \end{aligned}\right\} \tag{09}$$

The associated boundary conditions are

$$\left.\begin{array}{l} f(a)=\dfrac{\varpi a}{2}, f'(a)=\dfrac{\varpi}{2}, \vartheta(a)=1, N_{BM}\vartheta'(a)+N_{TP}h'(a)=0, m(a)=1 \\ f'\to\dfrac{1-\varpi}{2}, \vartheta\to 0, h\to 0, m\to 0 \ as\ \xi\to\infty \end{array}\right\} \quad (10)$$

The dimensionless parameters presented in (09-10) are

$$\left.\begin{array}{l} M_F=\dfrac{\sigma B_0^2}{2\left(\rho c_p\right)_{bf}U}, \delta=\dfrac{U_{in}}{U_w}, RD=\dfrac{16\sigma^* T_{in}^3}{3k\kappa_{bf}\left(\rho c_p\right)_{bf}}, Pr=\dfrac{\nu_{bf}}{\alpha_{bf}}, N_{BM}=\dfrac{\tau D_{BM}C_{in}}{\nu_{bf}}, \\ N_{TP}=\dfrac{\tau D_{TP}\left(T_w-T_{in}\right)}{T_{in}\nu_{bf}}, Le=\dfrac{\alpha_{bf}}{D_{BM}}, Lb=\dfrac{\alpha_{bf}}{D_{MO}}, Pe=\dfrac{bW_c}{D_{MO}}, \Upsilon=\dfrac{M_{in}}{M_w-M_{in}}, \varpi=\dfrac{U}{U_w} \end{array}\right\} (11)$$

Also, the reduced dimensionless physical quantities are

Skin friction $Cfr=\dfrac{(8a)^{0.5}f''(a)}{(1-\varphi_1)^{2.5}(1-\varphi_2)^{2.5}}$

Nusselt number, $Nur=-\dfrac{\kappa_{hnf}}{\kappa_{bf}}a^{0.5}(2+RD)\vartheta'(a)$

Sherwood number for nanoparticles, $Shr=-2a^{0.5}h'(a)$

Microorganism's number, $Mor=-2a^{0.5}m'(a)$

5.2 SOLUTION TECHNIQUES:

The changed overseeing Conditions (09) alongside the limit conditions (10) are switched over completely to introductory worth issue and are tackled utilizing RKF-45 strategy with the assistance of shooting method

$$\begin{bmatrix} f & \vartheta & h & m \\ f' & \vartheta' & h' & m' \\ f'' & \vartheta'' & h'' & m'' \\ f''' & 0 & 0 & 0 \end{bmatrix}=\begin{bmatrix} d_1 & d_4 & d_6 & d_8 \\ d_2 & d_5 & d_7 & d_9 \\ d_3 & d_5' & d_7' & d_9' \\ d_3' & 0 & 0 & 0 \end{bmatrix} \quad (12)$$

Using the above relations, the Equations (09)are converted to first order equations as follows:

$$\begin{pmatrix} d_1' \\ d_2' \\ d_3' \\ d_4' \\ d_5' \\ d_6' \\ d_7' \\ d_8' \\ d_9' \end{pmatrix} = \begin{pmatrix} d_2 \\ d_3 \\ -\frac{1}{\xi}\left[d_3 + \frac{1}{2\frac{\mu_{hnf}}{\mu_{bf}}\left(1+\beta^{-1}\right)}\left\{ \frac{\rho_{hnf}}{\rho_{bf}} d_1 d_2 - \frac{\sigma_{hnf}}{\sigma_{bf}} M_F \left(d_2 - \delta \right) \right\} \right] \\ d_5 \\ -\frac{1}{\xi}\left[d_5 + \frac{Pr}{\left(2+RD\right)} \frac{\kappa_{bf}}{\kappa_{hnf}} \frac{\left(\rho c_p\right)_{hnf}}{\left(\rho c_p\right)_{bf}} \left\{ d_1 d_5 + 2\xi \left(N_{BM} d_5 d_7 + N_{TP} d_5^{\,2} \right) \right\} \right] \\ d_7 \\ -\frac{1}{2\xi}\left\{ 2d_7 + Le.d_1 d_7 + 2\frac{N_{TP}}{N_{BM}} \left(\xi d_5' + d_5 \right) \right\} \\ d_9 \\ -\frac{1}{2\xi}\left[2d_9 + Pr.Lb.d_1 d_9 - Pe\left\{ 2\xi \left(d_7 d_9 + d_8 d_7' + \Upsilon d_7' \right) + \left(d_8 + \Upsilon \right) d_6 \right\} \right] \end{pmatrix} \quad (13)$$

The associated initial conditions are

$$\left.\begin{aligned} &d_1(a) = \frac{\varpi a}{2}, d_2(a) = \frac{\varpi}{2}, d_3(a) = \alpha_1, d_4(a) = 1, d_5(a) = \alpha_2, \\ &d_6(a) = \alpha_3, d_7(a) = -\frac{N_{BM}}{N_{TP}} \alpha_2, d_8(a) = 1, d_9(a) = \alpha_4 \end{aligned}\right\} \quad (14)$$

In the beginning of value line item (1), five cases are known and therefore a surplus using shooting method remains outstanding. Subsequent to, setting the boundaries for far field limit conditions perform estimations and tackled by using request optics RK-45 process with. Finally this method determines the valid step size and at every interval it estimates analysis two times. If these two estimates are in close agreement with each other, it is accepted. Otherwise, the step size is reduced further and calculation repeated until desired accuracy reached. The results are confirmed by comparing it with the recent literature and the comparison is shown in Table 3.

Table 03: Validation of results

Pr	$\vartheta'(0.1)$		
	Qasim et al. [53]	Suleman et al. [54]	Present work

0.72	1.23664	1.23665	1.23665
1	1.0	1.0	1.0
6.7	0.3333	0.33331	0.33332
10	0.26876	0.26877	0.26876

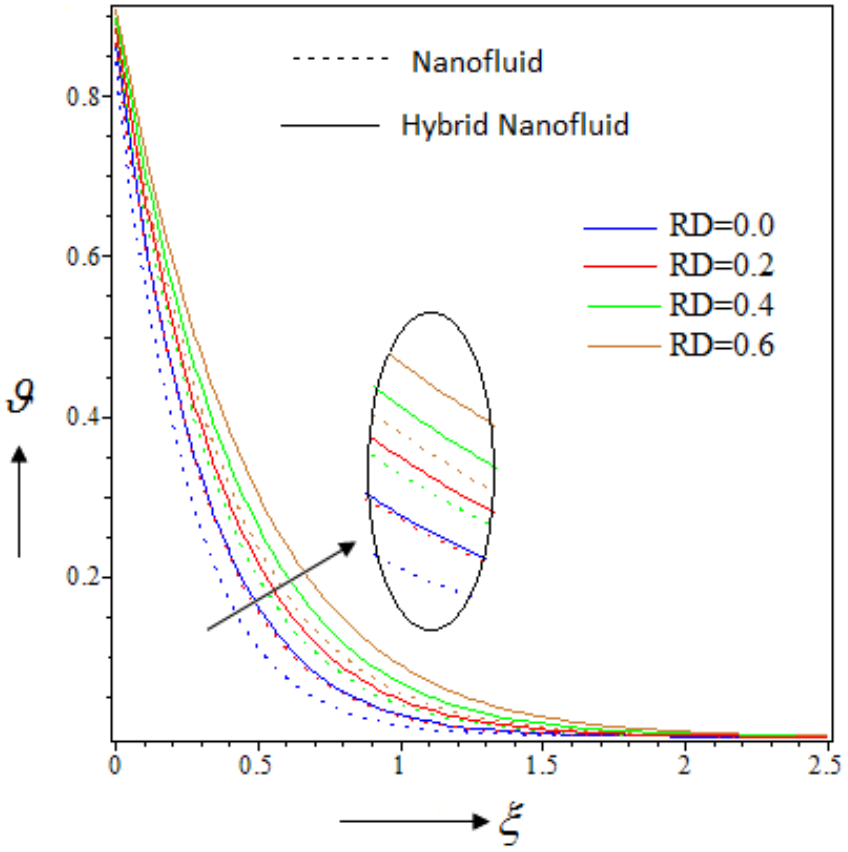

Figure 02: Effects of RD on $\vartheta(\xi)$

5.3 RESULT AND DISCUSSIONS:

We have investigated the effects of various barriers on the temperature, focus, and thickness profile of the microorganisms by mathematical simulations. The outcomes are acquired as diagrams outlines including the way of behaving of skin grinding coefficient, Nusselt number, and motile thickness number. We are centered on the examination of the outcomes between Ag/H_2O nanofluid and $Ag+TiO_2/H_2O$ hybrid nanofluid.

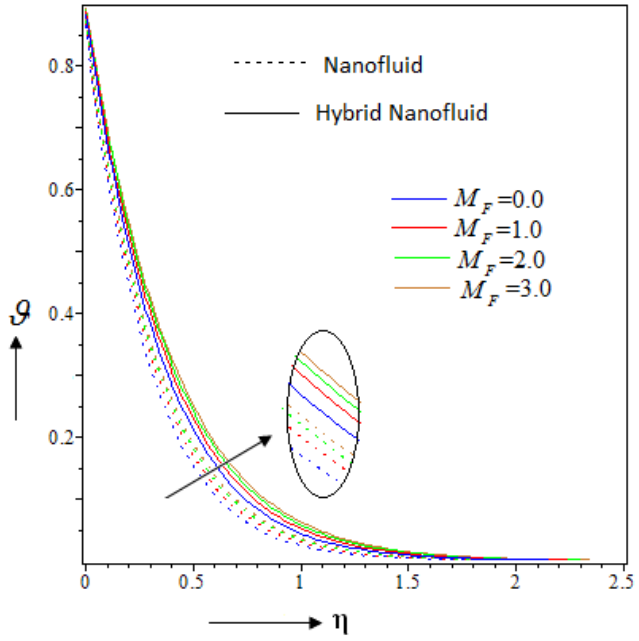

Figure 03: Effects of M_F on $\vartheta(\xi)$

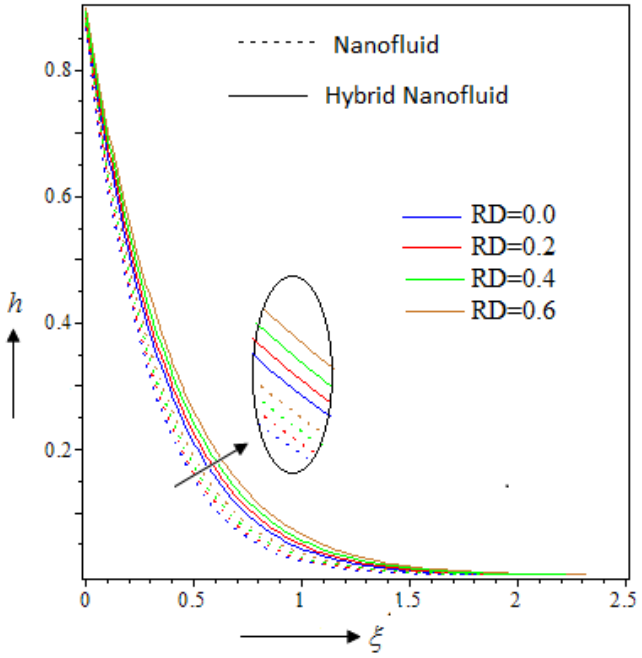

Figure 04: Effects of RD on $h(\xi)$

First, we look at how the radiation boundary affects the temperature at which nanofluid and cross-breed nanofluid progress. The temperature of the stream rises in response to high radiation levels, as Figure 02 illustrates.

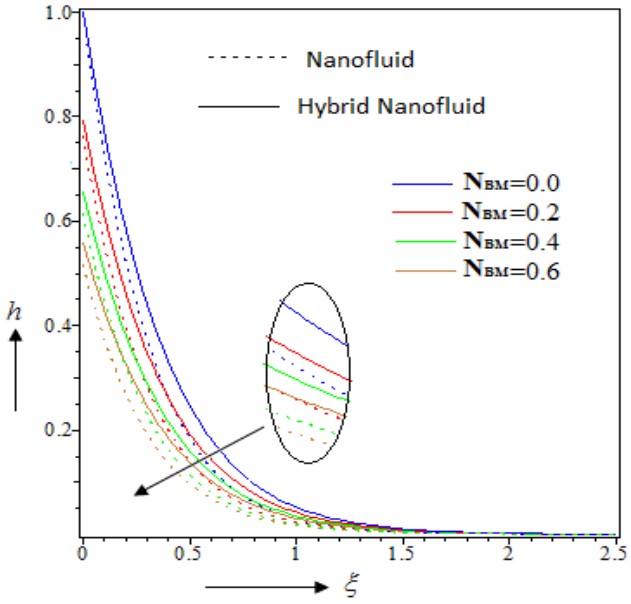

Figure 05: Effects of N_{BM} on $h(\xi)$

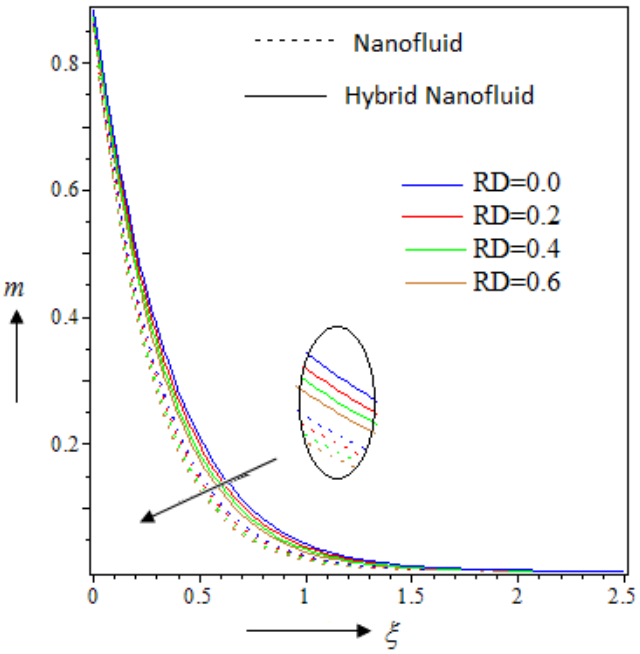

Figure 06: Effects of RD on $m(\xi)$

However, it is worth focusing on that in the event of half breed nanofluid stream it answers more noticeably to the radiation than that of nanofluid stream. Additionally, with the higher separation from the outer layer of the stream, the temperature of the stream framework steadily and reliably diminishes to nothing.

Comparable impact is seen in the event of impact of attractive boundary on the temperature of the stream in figure 03. Here we witness that higher attractive power implies higher Lorentz force that impedes the progression of the liquid which gives the nanoparticles to retain additional intensity energy from the stream surface and in this way it expands the temperature of the stream. We likewise witness that mixture nanoparticles are more effectively equipped for engrossing intensity than nanoparticle. The influence of radiation on the nanoparticle thickness is organized I figure 04. It is perceptibly upgraded with higher radiation close to the outer layer of the stream.

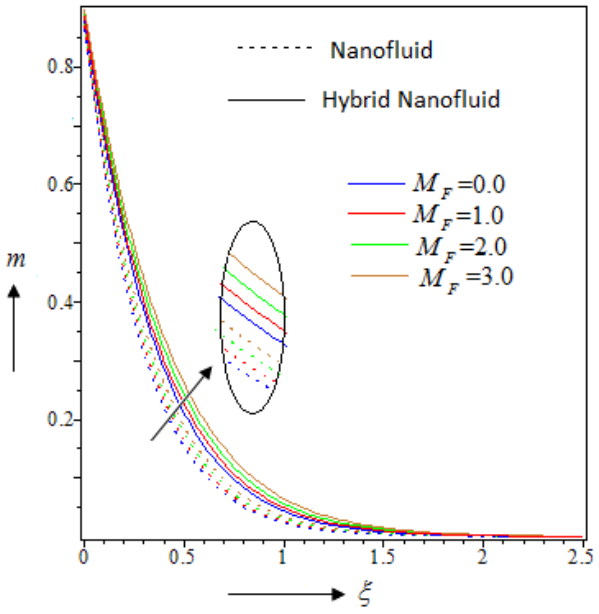

Figure 07: Effects of M_F on $m(\xi)$

Additionally, we are keen on working out the impacts of Brownian movement factor on the nanoparticle thickness as introduced in figure 00 Here it is fascinating to see that raised arbitrary development of the nanoparticle reduces the nanoparticle thickness close to the surface, yet in the event of half and half nanofluid its thickness diminishes less. In figure 06-07, how is the microorganism thickness affected by the radiation and attractive power?

Table 04: Values of physical quantities subject to the various factors

RD	M_F	*Cfr*		*Nur*		*Shr*		*Mor*	
		Ag/H_2O	$Ag+TiO_2/H_2O$	Ag/H_2O	$Ag+TiO_2/H_2O$	Ag/H_2O	$Ag+TiO_2/H_2O$	Ag/H_2O	$Ag+TiO_2/H_2O$
0.0	1.0	0.124536	0.102345	7.501215	8.611254	2.456589	2.699871	0.822359	1.335473
0.1		0.234415	0.217845	6.998548	8.120245	2.211547	2.522130	1.022358	1.640012

0.2		0.354568	0.345156	6.500568	7.588941	2.012456	2.294578	1.233456	1.822457
0.3		0.445781	0.441215	0955648	7.025480	1.800234	2.012457	1.414567	2.100245
0.4		0.562314	0.558978	0421665	6.523012	1.700254	1.855648	1.65478	2.388457
0.2	0.0	0.361247	0.360012	4.901257	0811248	0.122345	0.522135	1.855791	2.014789
	0.5	0.347784	0.341542	0622315	6.455218	0.645791	1.244518	1.544781	1.911012
	1.0	0.354568	0.345156	6.500568	7.588941	2.012456	2.294578	1.233456	1.822457
	1.5	0.334518	0.330012	7.001245	8.124580	3.511249	3.800124	1.044215	1.644578
	2.0	0.301245	0.300008	7.611487	8.897513	4.945487	0266489	0.812254	1.500248

At the point when we increment the radiation in the outer layer of the stream, we see that microorganisms are swimming away from the superficial because of the expanded temperature in the stream. Be that as it may, it is

getting increasingly dense if there should arise an occurrence of higher attractive power field.

The impacts of radiation and attractive power on the actual amounts of the stream in organized in table 04. The radiation expands the skin rubbing of the stream, which brings about lessened intensity and mass exchange of the nanoparticle. However, if there should arise an occurrence of microorganism move rate, it lifts with higher radiation. Additionally, because of less skin grating in half breed nanofluid stream, intensity and mass exchange rate is a lot higher than that of nanofluid stream. With regards to the attractive power impact on the stream, it decreases the skin erosion of the stream thus the intensity and mass exchange rate is raised with more grounded attractive field in the stream. Be that as it may, microorganism move rate is decreased with an ever increasing number of attractive fields.

5.4 CONCLUDING REMARKS:

Radiation, magnetic fields, and nanofluid properties are the most critical variables in heat and mass transfer processes, according to the study. Nanofluids with enhanced thermal and convective properties are called hybrid nanofluids. As a result, they guarantee superior performance in comparison to standard nanofluids. In light of the critical examination that was conducted on the bioconvective Casson flow of hybrid nanofluid that included gyrotactic microorganisms across a thin and slender needle, the following major discoveries were made:

- The introduction of radiation into a fluid's flow raises its temperature and enhances its mass and heat transfer rates. Particularly in the case of hybrid nanofluids, which outperform their single-component counterparts in terms of efficiency.

- Radiation strengthens the overall thermal behavior of the fluid; thus, hybrid nanofluids become more effective in those applications which require enhanced thermal management.
- The temperature and concentration of microorganisms in the fluid rise when an external magnetic field is applied. However, its impact on the concentration of nanoparticles is essentially insignificant. These data indicate that biological components in the fluid are highly affected by magnetic fields, while the distribution pattern of nanoparticles is less directly affected.
- A lower skin friction coefficient for a fluid is seen with stronger magnetic fields. Consequently, the rate of mass and heat transfer for nanoparticles is accelerated by this decline. A strong magnetic field improves the efficiency of mass and heat transmission in a fluid.
- The mass transfer rate is thought to show a pattern in radiation fluctuation and magnetic field variation that is in contradiction to one another. This reflects that the interaction between the two abovementioned physical factors differently affects the motion and effectiveness of microorganisms. While radiation generally increases the mass transfer rate, a magnetic field does it differently. This develops complex behavior patterns in the bioconvection processes.
- Compared to nanofluids made of single components, hybrid nanofluids have consistently demonstrated superior performance in terms of mass transfer and heat enhancement. Hybrid nanofluids are proven useful in applications requiring high heat and mass transfer requirements because they incorporate many types of nanoparticles, resulting in improved thermal and transport characteristics.

REFERENCES:

[1] JR.Platt, " bioconvection patterns" in cultures of free-swimming organisms. Science, Vol 2,Page:133(3466), 1961

[2] S .Ghorai, NA Hill. “Wavelengths of gyrotactic plumes in bioconvection”. Bulletin of mathematical biology. May;Vol 62(3):Page:429-50. 2000

[3] SU.Choi, A. Jeffrey “Eastman, enhancing thermal conductivity of fluids with nanoparticles”. InASME international mechanical engineering congress & exposition Nov,Vol 23 (page. 12-17). 1995

[4] Y.Xuan, W Roetzel. “Conceptions for heat transfer correlation of nanofluids”. International Journal of heat and Mass transfer Oct Vol 1;43(19):3701-7, 2000

[5] Y Xuan, Q Li. “Heat transfer enhancement of nanofluids”. International Journal of heat and fluid flow. Feb Vol 1,21(1):Page:58-64. 2000

[6] Sinha A, Misra JC. “Effect of induced magnetic field on magnetohydrodynamic stagnation point flow and heat transfer on a stretching sheet”. Journal of Heat Transfer. Nov 1;136(11). 2014

[7] Basir ,M. Uddin ,M. Ismail , “Unsteady magnetoconvective flow of bionanofluid with zero mass flux boundary condition. Sains Malaysiana”. Feb 1;Vol:46(2),Page:327-33,2017

[8] Reddy, NB. Poornima, T. Sreenivasulu , “ Radiative heat transfer effect on MHD slip flow

of Dissipating Nanofluid past an exponential stretching porous sheet". Int. J. Pure Appl. Math.;Vol:109(9):Page:134-42. 2016

[9] Sreenivasulu, P. Poornima, T. Bhaskar Reddy, " Thermal radiation effects on MHD boundary layer slip flow past a permeable exponential stretching sheet in the presence of joule heating and viscous dissipation". Journal of Applied Fluid Mechanics. Dec 1;Vol:9(1),Page:267-78. 2015

[10]Parida SK, Panda S, Rout BR, "MHD boundary layer slip flow and radiative nonlinear heat transfer over a flat plate with variable fluid properties and thermophoresis", Alexandria Engineering Journal. Dec 1;Vol:54(4),Page:941-53. 2015

[11]Nayak ,MK. Shaw, S.Chamkha, " Impact of variable magnetic field and convective boundary condition on a stretched 3D radiative flow of Cu-H2O nanofluid". AMSE JOURNALS-AMSE IIETA Series: Modelling B.;Vol:86(3),Page:658-678.2018

[12]Nayak, MK.Akbar, NS. Tripathi D, Pandey VS, " Three dimensional MHD flow of nanofluid over an exponential porous stretching sheet with convective boundary conditions", Thermal Science and Engineering Progress. Vol:54(4),Page:941-53. 2017

[13]F. Mabood, W. A. Khan, A.I.M. Ismail, "Multiple slips effects on MHD Casson fluid flow in porous media with radiation and chemical reaction", Canadian Journal of Physics, Vol:94(1),Page: 26-34, 2016.

[14]D.A. Nield, A.V. Kuznetsov, "The Cheng–Minkowycz problem for natural convective boundary-layer flow in a porous medium saturated by a nanofluid", International Journal of Heat and Mass Transfer, Vol:52, Page 5792-5795, 2009.

[15]M. Turkyilmazoglu, "Fluid flow and heat transfer over a rotating and vertically moving disk", Physics of Fluids,Vol: 30, Page:56, 2018.

[16]K. Das, "Slip flow and convective heat transfer of nanofluids over a permeable stretching surface", Computers and Fluids,Vol: 64,Page: 34–42, 2012.

[17]T. Hayat, A. Kiran, M. Imtiaz, A. Alsaedi, "Melting heat and thermal radiation effects in stretched flow of an Oldroyd-B fluid", Applied Mathematics and Mechanics,Vol: 38(7),Page: 957-968, 2017.

[18]J. Sui, L. Zheng, X. Zhang, "Boundary layer heat and mass transfer with Cattaneo- Christov double diffusion in upper-convected Maxwell nanofluid past a stretching sheet with slip velocity", International Journal of Thermal Sciences,Vol: 104,Page: 461-468, 2016.

[19]T. Hayat, M. Imtiaz, A. Alsaedi, "Effects of homogeneous–heterogeneous reactions in flow of Powell–Eyring fluid", Journal of Central South University, Vol:22 (8),Page: 3211–3216, 2010

[20]G. Aaiza, I. Khan, S. Shafie, "Energy transfer in mixed convection MHD flow of nanofluid containing different shapes of nanoparticles in a channel filled with saturated porous medium", Nanoscale Research Letters, Vol:10,Page: 490, 2010

[21]N. Sandeep, "Effect of aligned magnetic field on liquid thin film flow of magnetic-nanofluids embedded with graphene nanoparticles", Advanced Powder Technology, Vol:28(3),Page: 865-875, 2017.

[22]Khan, WA. Makinde ,OD.Khan, "MHD boundary layer flow of a nanofluid containing

gyrotactic microorganisms past a vertical plate with Navier slip". International journal of heat and mass transfer. Jul 1;Vol:74,Page:285-91, 2014

[23]Gireesha, BJ. Kumar, KG Manjunatha , "Impact of chemical reaction on MHD 3D flow of a nanofluid containing gyrotactic microorganism in the presence of uniform heat source/sink". International Journal of Chemical Reactor Engineering. Dec 1;Vol:16(12), 2018

[24]Gireesha, BJ. Kumar, KG Manjunatha ,Manjunatha S. "Effect of viscous dissipation on three dimensional flow of a nanofluid by considering a gyrotactic microorganism in the presence of convective condition". InDefect and Diffusion Forum Trans Tech Publications Ltd. Vol. 388, Page:114-123,2018

[25]Hayat, T Nadeem, "Heat transfer enhancement with Ag–CuO/water hybrid nanofluid". Results in physics.Jan 1;Vol:7,Page:17-24., 2017

[26]Tayebi T, Chamkha AJ. "Entropy generation analysis due to MHD natural convection flow in a cavity occupied with hybrid nanofluid and equipped with a conducting hollow cylinder". Journal of Thermal analysis and Calorimetry. Feb;Vol:139(3),Page:2165-79., 2020

[27]Ghalambaz M, Doostani A, Izadpanahi E, Chamkha AJ. "Conjugate natural convection flow of Ag–MgO/water hybrid nanofluid in a square cavity". Journal of Thermal Analysis and Calorimetry.Feb;Vol:139(3),Page:2321-36, 2000

[28]Dogonchi AS, Nayak MK, Karimi N, Chamkha AJ, Ganji DD. "Numerical simulation of hydrothermal features of Cu–H2O nanofluid natural convection within a porous annulus considering diverse configurations of heater", Journal of Thermal Analysis and Calorimetry. Sep;Vol:141(5),Page:2109-20, 2010

[29]Manjunatha S, Kuttan BA, Jayanthi S, Chamkha A, Gireesha BJ. " Heat transfer enhancement in the boundary layer flow of hybrid nanofluids due to variable viscosity and natural convection" Heliyon. Apr 1;Vol:5(4):Page:01469, 2019

[30]Animasaun IL. "Dynamics of unsteady MHD convective flow with thermophoresis of particles and variable thermo-physical properties past a vertical surface moving through binary mixture", Open Journal of Fluid Dynamics.;Vol:5(02):Page:106, 2015

[31]Animasaun IL. "Effects of thermophoresis, variable viscosity and thermal conductivity on free convective heat and mass transfer of non-darcian MHD dissipative Casson fluid flow with suction and nth order of chemical reaction. Journal of the Nigerian Mathematical Society", Apr 1;Vol:34(1),Page:11-31,2015

[32]Sandeep, N. Koriko, OK. Animasaun IL. "Modified kinematic viscosity model for 3D-Casson fluid flow within boundary layer formed on a surface at absolute zero", Journal of Molecular Liquids. Sep 1,Vol;221,Page:1197-206, 2016

[33]Chaudhary MA, Merkin JH. "A simple isothermal model for homogeneous-heterogeneous reactions in boundary-layer flow. I Equal diffusivities", Fluid dynamics research. Nov 1;Vol:16(6),Page:311-33,1995

[34]Chaudhary ,MA. Merkin, “A simple isothermal model for homogeneous-heterogeneous reactions in boundary-layer flow”. II Different diffusivities for reactant and autocatalyst. Fluid dynamics research. Nov 30;Vol:16(6),Page:330, 1995

[35]Makinde, OD. Animasaun IL. “Bioconvection in MHD nanofluid flow with nonlinear thermal radiation and quartic autocatalysis chemical reaction past an upper surface of a paraboloid of revolution”, International Journal of Thermal Sciences. Nov 1;Vol:109,Page:159-71, 2016

[36]Lee LL., “Boundary layer over a thin needle”, The physics of fluids. Apr;Vol:10(4),Page:820-828, 1967

[37]Narain ,JP. Uberoi, “Combined forced and free-convection heat transfer from vertical thin needles in a uniform stream”, The Physics of Fluids. Nov;Vol:15(11),Page:1879-1882,1972

[38]Narain ,JP. Uberoi , “Combined forced and free-convection over thin needles”. International Journal of Heat and Mass Transfer.Aug 1;Vol:16(8),Page:1505-12,1973

[39]Chen ,JL. Smith,“Forced convection heat transfer from nonisothermal thin needles”,Vol: 33 Page:358-362, , 1978

[40]Ishak ,A.Nazar, R .Pop., “Boundary layer flow over a continuously moving thin needle in a parallel free stream”, Chinese Physics Letters. Oct 1;Vol:24(10),Page:2890 ,2017

[41]Ahmad, S. Arifin, NM. Nazar, R. Pop, “Mixed convection boundary layer flow along vertical thin needles: Assisting and opposing flows”. International Communications in Heat and Mass Transfer. Feb 1;Vol:35(2),Page:157-62, 2018

[42]Amirsom, NA. Uddin, MJ. Ismail, “MHD boundary layer bionanoconvective non-Newtonian flow past a needle with Stefan blowing”, Heat Transfer—Asian Research. Mar;Vol48(2),Page:727-43, 2019

[43]Tian, XY. Li, BW. Zhang, “The effects of radiation optical properties on the unsteady 2D boundary layer MHD flow and heat transfer over a stretching plate”, International Journal of Heat and Mass Transfer. Feb 1;Vol:105,Page:109-23, 2017